Using planning CTs to enhance CNN-based bladder segmentation on Cone Beam CT

Eliott Brion*, Jean Léger, Umair Javaid, John Lee, Christophe De Vleeschouwer, and Benoit Macq

Université catholique de Louvain, Louvain-la-Neuve, Belgium

ABSTRACT

For prostate cancer patients, large organ deformations occurring between the sessions of a fractionated radiotherapy treatment lead to uncertainties in the doses delivered to the tumour and the surrounding organs at risk. The segmentation of those structures in cone beam CT (CBCT) volumes acquired before every treatment session is desired to reduce those uncertainties. In this work, we perform a fully automatic bladder segmentation of CBCT volumes with u-net, a 3D fully convolutional neural network (FCN). Since annotations are hard to collect for CBCT volumes, we consider augmenting the training dataset with annotated CT volumes and show that it improves the segmentation performance.

Our network is trained and tested on 48 annotated CBCT volumes using a 6-fold cross-validation scheme. The network reaches a mean Dice similarity coefficient (DSC) of 0.801 ± 0.137 with 32 training CBCT volumes. This result improves to 0.848 ± 0.085 when the training set is augmented with 64 CT volumes. The segmentation accuracy increases both with the number of CBCT and CT volumes in the training set. As a comparison, the state-of-the-art deformable image registration (DIR) contour propagation between planning CT and daily CBCT available in RayStation reaches a DSC of 0.744 ± 0.144 on the same dataset, which is below our FCN result.

Keywords: Convolutional Neural Networks, Segmentation, Cone Beam CT, Radiotherapy, Bladder

1. INTRODUCTION

External beam radiation therapy (EBRT) treats cancer by delivering daily fractions of radiation to a tumor volume while attempting to spare normal tissues. Current techniques allow for planning and delivery of complex dose distributions in order to improve dose delivery in the target volume while better sparing surrounding healthy organs. At treatment planning, clinicians delineate the tumor and organs volumes on a computed tomography (CT) and compute the dose distribution. At treatment delivery, the patient is aligned with its treatment planning position and the dose fraction is delivered. Patient positioning relies on a daily cone beam computed tomography (CBCT) volume acquired in treatment position before each treatment fraction. Importantly, large day-to-day variations occur in the pelvic region due to matter income and outcome (e.g. bladder filling) and can impair treatment dose conformity.[1] Hence, anatomical variations detection (between planning and treatment stages) on the CBCT volume is needed. Current clinical practice includes it through a CBCT visual inspection but the automatic pelvic organs segmentation in daily CBCT volumes would allow an accurate measure of the anatomical variations and better prevent non-compliant dose delivery. The automation of the segmentation is required for an integration in the clinical workflow since manual organs delineation on daily volumes is too time-consuming. Our proposed approach focusses on the automatic bladder segmentation on CBCTs with u-net, a fully convolutional neural network. Since annotations are hard to collect for CBCT volumes, we consider augmenting the training dataset with annotated CT volumes following a supervised domain adaptation strategy.

Automatic organs segmentation in CBCT volumes is challenging due to poor soft tissue contrast and the various reconstruction artifacts.[2] Two main approaches have been previously proposed to tackle this. Classical clinically used segmentation methods include deformable image registration (DIR) methods between planning CT and daily CBCT volumes[3–5] to segment the bladder in CBCTs. Although it shows improvement compared to rigid

*The first two authors contributed equally. Send correspondence to Eliott Brion or Jean Léger: {eliott.brion,jean.leger}@uclouvain.be.

registration, a large proportion of the obtained bladder contours are unacceptable in case of large deformations between the registered volumes as in the pelvic region.[6] Statistical shape models[7] allow to capture shape variations and have been used for bladder segmentation on CBCT.[8,9] However, those methods require the definition of landmarks or meshes. Also, building a patient specific shape model[8] requires the availability of several delineated CBCT volumes, which is hampering the application from the start of the treatment. Alternatively, in order to limit the number of required delineated CBCT volumes while following the shape variation along a treatment, the model is best updated on segmentations manually corrected during the treatment.[9] However, this requires user intervention. Henceforth, none of these methods closes the challenging task of pelvic organs segmentation on CBCT volumes.

In parallel, the recent advances in computing capabilities, the availability of representative datasets and the high versatility of deep learning approaches allowed them to reach impressive segmentation performance, competing with state-of-the-art segmentation tools. In contrast with the above-mentioned segmentation techniques, deep learning algorithms are supposed to be robust to shape and appearance variations if those variations are captured in the training database and they do not require a landmarks definition. Deep learning algorithms have already been successfully used to segment pelvic organs on CT images, including the urinary bladder.[10,11] Hence, our goal is to perform fully automatic bladder segmentation in CBCT volumes with u-net, a 3D fully convolutional neural network (FCN).[12] To our knowledge, there has not been any attempt yet to use deep learning to segment the bladder in CBCTs, probably due to the scarcity of annotated data. In order to deal with of the small amount of annotated daily CBCT volumes, the performance improvement provided by the augmentation of the training dataset with annotated planning CT volumes is proposed. We motivate this choice by the fact that CBCT volumes can be roughly considered as noisy and distorted CT volumes in a segmentation perspective, hence sharing shape and contextual information with the CT volumes. We investigate the performance of u-net for different numbers of training CT and for different numbers of training daily CBCT, and show that adding CTs in the training set helps for contouring CBCTs.

Our approach is an instance of transfer learning and, more precisely, an instance of supervised domain adaptation. *Transfer learning* refers to the situation where a model is trained either (i) using data coming from different domains or (ii) on different tasks or (iii) both using data coming from different domains and on different tasks.[13] Our model is trained on two similar but different domains (CT and CBCT) on the same task (classifying each voxel of a 3D matrix as bladder on non-bladder). The CT domain is called *source* domain since it is the one from which most training data come, while the CBCT domain is called *target* domain since it is the one for which we want our model to perform well. As it is the case in most transfer learning applications, our source domain data are used to mitigate the small number of available target data during training. The situation where source and target domains are different is referred as *domain adaptation*, which is a subclass of transfer learning.[14] In our approach, all target data are labeled (i.e., we dispose of a contour of the bladder for all CBCTs) and therefore we are in the situation of *supervised domain adaptation*. Our approach shares similarities with Kamnitsas et al.,[15] where brain lesions are segmented using datasets coming from different domains. The key difference with our work is that their target domain data are unlabeled (i.e., they perform *unsupervised domain adaptation*). However, they compare their approach with a network jointly trained with labeled source and target data, which is more similar to our approach. Ghafoorian et al.[16] perform supervised domain adaptation to learn brain lesion segmentation on MRI across FLAIR and T1 images. However, they first pre-train the network on the source domain dataset before fine-tuning it on the target domain dataset. We jointly train our network on both source and target data.

In Section 2, we present both datasets of labeled CTs and CBCTs used in this study. We also introduce the u-net architecture, our learning strategy and the comparison baselines. In Section 3, we report the results and discuss them. Finally, we conclude in Section 4.

2. MATERIALS AND METHODS

In this section, we propose a method to assess whether adding CTs in the training set boosts the performance of a neural network to segment CBCTs. We use a dataset of 112 CTs and 48 CBCTs, presented in Section 2.1. These data are fed to the u-net neural network, whose architecture is described in 2.2. In order to evaluate the gain brought by CTs, we evaluate u-net's performance on a fixed dataset of 48 CBCTs in different training settings

(i.e., with a varying number of training CTs and training CBCTs). The cross-validation scheme detailed in Section 2.3 improves the statistical relevance of our results, mitigating the small size of our dataset. The performance metrics are defined in the same section. The performance of u-net in the different training settings is compared to other segmentation algorithms (using a commercial software on our data and reporting the results from other authors on other datasets) in Section 2.4.

2.1 Data and pre-processing

Our data consist of (i) a set $\mathcal{S}_1$ of 64 patients for which we have a CT which has been delineated by a trained expert and (ii) a set $\mathcal{S}_2$ of 48 patients (different from the 64 patients mentioned above) for which we have a planning CT and a daily CBCT (acquired with a Varian TrueBeam STx version 1.5), which have been both delineated by a trained expert. The patients of sets $\mathcal{S}_1$ and $\mathcal{S}_2$ respectively underwent EBRT at CHU-UCL-Namur and CHU-Charleroi Hôpital André Vésale. The use of these retrospective, anonymized data for this study has been approved by each hospital's ethics committee. In order to ensure data uniformity accross the entire dataset, all the 3D CT and CBCT volumes (as well as the 3D binary mask representing the ground truth segmentations) have been re-sampled on a 2x2x2 mm regular grid. Every re-sampled image volume and binary mask volume are cropped to volumes of 96x96x80 voxels centered on the bladder. Downsampling and cropping allow the model parameters, each batch of eight image volumes and the corresponding eight binary mask volumes to fit in a 11 Gb GPU.

2.2 Network architecture

The 3D u-net fully convolutional neural network is considered in this study. The network follows the same architecture (i.e. number and composition of layers) as in Ronneberger et al.,[12] where the 3x3 convolutions, the 2x2 max-pooling and the 2x2 up-conversion operations have been replaced by their 3x3x3 and 2x2x2 counterparts, as in Ciçek et al.[17] The network takes as input the 96x96x80 image volume and outputs a prediction for the bladder segmentation. The input goes through a contracting path to capture context and an expanding path to enable precise localization. In the contracting path, a collection of features are learned thanks to successive convolutions and max-pooling operations. Successively, two 3x3x3 convolutions, followed by a ReLu activation, are applied before applying a 2x2x2 max-pooling. After each max-pooling step, the number of feature maps is doubled in order to allow the network to learn many high level features. Within a layer, the number of feature maps is kept constant as in Ronneberger et al.,[12] starting with 16 feature maps in the first layer. From the features learned in the contracting path, the expanding path increases the resolution via skip connections, successive 2x2x2 up-conversion operations, 3x3x3 convolutions and ReLu activations in order to recover the original volume size. In the last layer, a sigmoid is applied and the network outputs the probability for each voxel to belong to the bladder. To obtain the final binary segmentation mask, a threshold of 0.5 is chosen. The network is trained with the Dice loss. The optimization algorithm used is Adam with learning rate 10^{-4} and a batch size of 8. We use the validation set to earlystop the training (with a maximum of 100 epochs). Training data (both CBCT and CT image volumes as well as their binary mask volumes) are augmented using rotation (comprised between $-5°$ and $5°$ along each of the three axes), shift (comprised between -5 and 5 pixels along each axes) and shear (reasonable values for the affine transformation matrix).

2.3 Learning strategy and performance assessment

In the rest of this paper, a "CT volume" (or "CBCT volume") refers to a couple of both the 3D image and the 3D binary mask representing the bladder segmentation on this image. We perform a six-fold cross-validation (see Table 1) with the 48 CBCT volumes of set $\mathcal{S}_2$, where four folds ($n_{CBCT} \leq 32$ volumes in total) are used as training set, one fold (8 volumes) is used as validation set for earlystopping and one fold (8 volumes) is used as test set. As shown in Figure 1, the number of training CBCT volumes n_{CBCT} has been varied such that $n_{CBCT} \in \{2, 4, 8, 16, 32\}$ by excluding a part of the 32 available volumes. The training set has been augmented with n_{CT} annotated CT volumes from set $\mathcal{S}_1$ such that $n_{CT} \in \{0, 16, 32, 64\}$. The same CT volumes are added to the CBCT training volumes independently on the four considered training folds. Hence, the training set contains $n_{CBCT} + n_{CT}$ volumes in total. Note that no CT volumes are present in the validation and test sets (indeed our goal is only to segment CBCT volumes). In order to evaluate our results, we use three metrics: the Dice similarity coefficient (DSC) and the Jaccard index (JI) measure the overlap between two binary masks, while the

symmetric mean boundary distance (SMBD) assesses the distance between the contours (i.e. the sets of points located at the boundary of the binary masks) extracted from those binary masks. More specifically,

$$\text{DSC} = \frac{2|A \cap B|}{|A| + |B|}, \tag{1}$$

$$\text{JI} = \frac{|A \cap B|}{|A \cup B|}, \tag{2}$$

$$\text{SMBD} = \frac{\overline{D}(A,B) + \overline{D}(B,A)}{2}, \tag{3}$$

where A and B are the predicted and reference segmentation binary masks, $D(A,B) = \{\min_{x \in \Omega_B} ||x-y||, y \in \Omega_A\}$ and Ω_A, Ω_B are respectively the contours extracted from A and B.

$\mathcal{S}_1$	$\mathcal{S}_2$ (CBCT)					
(CT)	fold1	fold2	fold3	fold4	fold5	fold6
train	train	train	train	train	*val*	**test**
train	train	train	train	*val*	**test**	train
train	train	train	*val*	**test**	train	train
train	train	*val*	**test**	train	train	train
train	*val*	**test**	train	train	train	train
train	**test**	train	train	train	train	*val*

Table 1. Six-fold cross-validation. To train the model, we use n_{CT} volumes from $\mathcal{S}_1$ and we use the n_{CBCT} first volumes from the CBCT folds labeled with "train". To earlystop the training, we use all eight volumes from the CBCT fold labeled with "val". To test the model, we use all eight volumes from the CBCT fold labeled with "test".

2.4 Comparison baselines

The prediction performed by our network is compared to several baselines. A first baseline has been obtained on the dataset presented in Section 2.1 by using the built-in contour propagation tool of RaySearch (RayStation* version 5.99.50.22). The contours from the planning CT volumes of set $\mathcal{S}_2$ have been propagated to the daily CBCT image volumes of the same patient by using a rigid registration followed by a regularized intensity-based deformable image registration (DIR). More precisely, the DIR algorithm is the ANACONDA algorithm,[18] where no controlling regions of interest (ROI) have been used, apart from the external/whole body structure. This follows the approach proposed in Takayama et al.[5] when no controlling ROIs (i.e. annotations) are available on the CBCT image volumes for the bladder (or other organs).

Additional baselines are reported on others CT-CBCT datasets obtained with different acquisition machines. A rigid registration followed by an intensity-based DIR between pairs of planning CT image volumes and daily CBCT image volumes is performed in Thor et al. (demon algorithm)[3] and Takayama et al. (ANACONDA algorithm without controlling ROIs).[5] In Woerner et al.,[4] several mutual information-based DIRs are performed after the rigid registration with a user intervention at the end of the process in order to tune a final DIR.

A patient specific bladder deformation model is proposed in Chai et al.[8] and van de Schoot et al.[9] In Chai et al.,[8] five delineated CBCT volumes serve as training data in order to build a statistical bladder shape model through principal component analysis (PCA) on shape vectors capturing the 3D position of 2091 landmarks on the bladder contour. Then, the test volume segmentation is obtained by deforming a reference segmentation (namely one of the training contours) along the major deformation modes obtained with PCA. This is done by the minimization of the absolute difference between the directional intensity gradients evaluated on the bladder contour in the reference CBCT and the bladder contour candidate in the test CBCT. In van de Schoot et al.,[9]

*https://www.raysearchlabs.com/raystation/.

the statistical shape model is built on two planning CT volumes instead of five treatment CBCT and updated on manually corrected contours during the treatment. The absolute difference minimization is also replaced by a cross-correlation maximization.

3. RESULTS AND DISCUSSION

In Figure 1, the DSC between the output segmentation of the FCN and the ground truth segmentation are computed and averaged over all 48 CBCT volumes from the six test folds. This is done for different numbers of training CBCTs and different numbers of training CTs. Those results are compared with the DIR algorithm of RayStation. Table 2 provides the mean and the standard deviation of the DSC, JI and SMBD for different numbers of training CBCT volumes and different numbers of training CT volumes. A mixed model with a random intercept on the patient showed significant difference between the algorithms' performance regarding their DSC ($p < 10^{-3}$), JI ($p < 10^{-3}$) and SMBD ($p < 10^{-3}$). The following three observations can be done based on Figure 1 and Table 2.

- The more CBCT volumes in the training set, the higher the DSC on the test set. A Tukey's range test performed on DSC reveals that Ours(32,0) performs significantly better than Ours(8,0) ($p < 10^{-3}$) and that Ours(32,64) performs significantly better than Ours(8,64) ($p < 10^{-3}$). This means that adding new CBCT volumes allows the network to better generalize on test set. This makes sense since the added training data and the test data are of the same modality (CBCT).
- Interestingly, the more CT volumes in the training set, the higher the mean DSC (Ours(8,64)>Ours(8,0) with $p < 10^{-3}$ and Ours(32,64)>Ours(32,0) with $p < 10^{-2}$). We explain this improvement by the learning of more generic features, leading to better generalization. However, the more training CBCT volumes, the smaller the gain obtained from additional CTs in the training set.
- When all available CT and CBCT volumes are used for training (32 CBCT volumes and 64 CT volumes), our approach outperforms the DIR algorithm of RayStation (Ours(8,64)>RayStation with $p < 10^{-3}$). This is illustrated on a representative patient in Figure 2. Our approach also outperforms the DSC metrics presented in Thor et al. on a different but comparable dataset. Note that those two DIR-based comparison baselines perform similarly, which suggests that our dataset is of similar difficulty than the one used by Thor et al. Our method also outperforms the results of Takayama et al. when their algorithm is used without controlling ROIs. Our method reaches results comparable to Woerner et al. but does not require a user intervention and the prediction requires a single pass in the CNN compared to a 6-pass deformable registration in Woerner et al. Although our algorithm performs worse than the one proposed by Chai et al. and van de Schoot et al., it is not patient specific. Hence, it does not require the availability of patient specific CBCT (or CT) contours beforehand, nor a model update during the treatment.

Although this discussion is based on the DSC, basing it on the JI or on the SMBD leads to the same observations with the same levels of confidence. From those observations, we conclude that our FCN outperforms alternative fully-automatic approaches and is slightly worse than a semi-automatic approach. Furthermore, adding in the training set volumes from a distribution (CT) different but close to the distribution of the test set (CBCT) improves the FCN performance.

4. CONCLUSION

The contribution of this paper is twofold. (i) To the best of our knowledge, this is the first attempt to use convolutional neural networks to segment the bladder on CBCT. (ii) We show that including in the training set volumes from a distribution (CT) close but different from the test set distribution (CBCT) improves the performance on this test set for the task at hand. Our proposed learning strategy leverages largely available labeled CT volumes available from radiotherapy planning to outperform current state-of-the-art DIR-based bladder segmentation on CBCT.

Convolutional neural networks result in accurate segmentation of the bladder for CBCT volumes. Moreover, we demonstrate that augmenting the training set with CT volumes (which are more accessible since labeling them

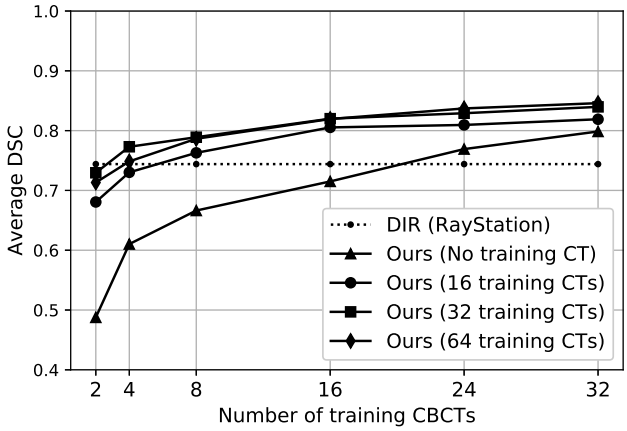

Figure 1. Influence of the number of the training CBCTs and CTs on the segmentation accuracy. DSC: Dice similarity coefficient.

Algorithm (n_{CBCT}, n_{CT})	DSC	JI	SMBD (mm)
Ours (8,0)	.669 ± .155	.521 ± .159	6.5 ± 3.1
Ours (8,64)	.788 ± .110	.663 ± .136	3.9 ± 1.9
Ours (32,0)	.801 ± .137	.685 ± .147	3.9 ± 2.6
Ours (32,64)	**.848 ± .085**	**.745 ± .114**	**2.8 ± 1.4**
DIR, RayStation	.744 ± .144	.612 ± .167	5.0 ± 3.1
DIR, Takayama et al. (2017)[5]*	.69 ± .07	-	-
DIR, Woerner et al. (2017)[4]*	∼ .83	-	-
PSM, van de Schoot et al. (2014)[9]*	∼ .87	-	-
PSM, Chai et al. (2012)[8]*	-	.785	-
DIR, Thor et al. (2011)[3]*	.73	-	-

Table 2. Comparison between our proposed algorithm in different settings (number of training CBCT volumes, number of training CT volumes) and the baseline algorithms regarding to overlap (DSC, JI) and distance (SMBD) measures. DSC: Dice similarity coefficient, JI: Jaccard index, SMBD: Symmetric mean boundary distance, DIR: Deformable image registration, PSM: Patient specific model. *Evaluated on a dataset different from ours.

is part of clinical practice, in contrary to CBCTs) improves the segmentation performance. Our FCN could be used in radiotherapy to precisely localize the bladder, allowing to reduce the dose delivered to this healthy organ in patients treated for prostate cancer. In future works, we could attempt to explain how deep features of CBCTs are improved by CT training data. Further analysis could also investigate how the information present in the annotated planning CT of a given patient can be leveraged to segment the subsequent CBCTs of the same patient.

ACKNOWLEDGMENTS

Eliott Brion's work was supported by FEDER-RW project UserMEDIA, Jean Léger is a Research Fellow of the Fonds de la Recherche Scientifique - FNRS, Umair Javaid is a Research Fellow funded by the F.N.R.S. Televie grant no. 7.4625.16, John A. Lee and Christophe De Vleeschouwer are Senior Research Associates with the Belgian F.R.S.-FNRS. We thank CHU-UCL-Namur (Dr Jean-François Daisne) as well as CHU-Charleroi (Dr Nicolas Meert) for providing the data. We thank Sara Teruel Rivas for her expertise in contouring CBCT images under supervision of Dr Laurette Renard.

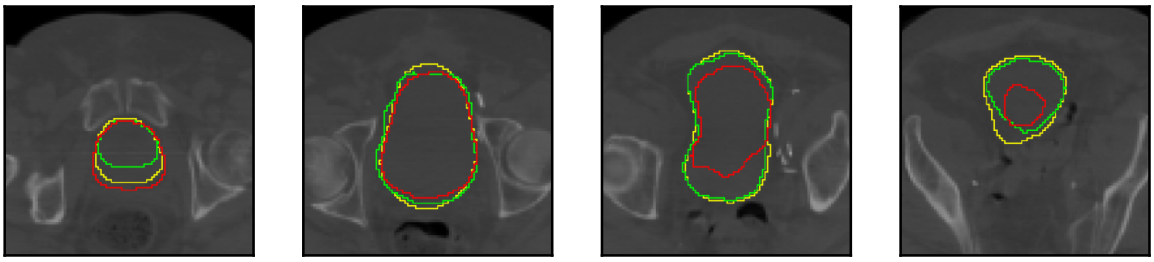

Figure 2. Comparison between the ground truth segmentation (in yellow), the DIR with RayStation segmentation (in red, DSC = 0.788) and our segmentation (in green, DSC = 0.892, setting $n_{CBCT} = 32$ and $n_{CT} = 64$) for a given patient. Each image represents a different slice of the same CT volume. DIR: Deformable image registration.

REFERENCES

[1] Peng, C., Ahunbay, E., Chen, G., Anderson, S., Lawton, C., and Li, X. A., "Characterizing interfraction variations and their dosimetric effects in prostate cancer radiotherapy," *International Journal of Radiation Oncology* Biology* Physics* **79**(3), 909–914 (2011).

[2] Weiss, E., Wu, J., Sleeman, W., Bryant, J., Mitra, P., Myers, M., Ivanova, T., Mukhopadhyay, N., Ramakrishnan, V., Murphy, M., et al., "Clinical evaluation of soft tissue organ boundary visualization on cone-beam computed tomographic imaging," *International Journal of Radiation Oncology* Biology* Physics* **78**(3), 929–936 (2010).

[3] Thor, M., Petersen, J. B., Bentzen, L., Høyer, M., and Muren, L. P., "Deformable image registration for contour propagation from ct to cone-beam ct scans in radiotherapy of prostate cancer," *Acta Oncologica* **50**(6), 918–925 (2011).

[4] Woerner, A. J., Choi, M., Harkenrider, M. M., Roeske, J. C., and Surucu, M., "Evaluation of deformable image registration-based contour propagation from planning ct to cone-beam ct," *Technology in cancer research & treatment* **16**(6), 801–810 (2017).

[5] Takayama, Y., Kadoya, N., Yamamoto, T., Ito, K., Chiba, M., Fujiwara, K., Miyasaka, Y., Dobashi, S., Sato, K., Takeda, K., et al., "Evaluation of the performance of deformable image registration between planning ct and cbct images for the pelvic region: comparison between hybrid and intensity-based dir," *Journal of radiation research* **58**(4), 567–571 (2017).

[6] Zambrano, V., Furtado, H., Fabri, D., Lütgendorf-Caucig, C., Góra, J., Stock, M., Mayer, R., Birkfellner, W., and Georg, D., "Performance validation of deformable image registration in the pelvic region," *Journal of radiation research* **54**(suppl_1), i120–i128 (2013).

[7] Heimann, T. and Meinzer, H.-P., "Statistical shape models for 3D medical image segmentation: a review," *Medical image analysis* **13**(4), 543–563 (2009).

[8] Chai, X., van Herk, M., Betgen, A., Hulshof, M., and Bel, A., "Automatic bladder segmentation on cbct for multiple plan art of bladder cancer using a patient-specific bladder model," *Physics in Medicine & Biology* **57**(12), 3945 (2012).

[9] van de Schoot, A., Schooneveldt, G., Wognum, S., Hoogeman, M., Chai, X., Stalpers, L., Rasch, C., and Bel, A., "Generic method for automatic bladder segmentation on cone beam ct using a patient-specific bladder shape model," *Medical physics* **41**(3) (2014).

[10] Kazemifar, S., Balagopal, A., Nguyen, D., McGuire, S., Hannan, R., Jiang, S., and Owrangi, A., "Segmentation of the prostate and organs at risk in male pelvic CT images using deep learning," *arXiv preprint arXiv:1802.09587* (2018).

[11] Cha, K. H., Hadjiiski, L., Samala, R. K., Chan, H.-P., Caoili, E. M., and Cohan, R. H., "Urinary bladder segmentation in ct urography using deep-learning convolutional neural network and level sets," *Medical physics* **43**(4), 1882–1896 (2016).

[12] Ronneberger, O., Fischer, P., and Brox, T., "U-net: Convolutional networks for biomedical image segmentation," in [*International Conference on Medical image computing and computer-assisted intervention*], 234–241, Springer (2015).

[13] Pan, S. J., Yang, Q., et al., "A survey on transfer learning," *IEEE Transactions on knowledge and data engineering* **22**(10), 1345–1359 (2010).

[14] Jiang, J., "A literature survey on domain adaptation of statistical classifiers," *URL: http://sifaka. cs. uiuc. edu/jiang4/domainadaptation/survey* **3**, 1–12 (2008).

[15] Kamnitsas, K., Baumgartner, C., Ledig, C., Newcombe, V., Simpson, J., Kane, A., Menon, D., Nori, A., Criminisi, A., Rueckert, D., et al., "Unsupervised domain adaptation in brain lesion segmentation with adversarial networks," in [*International Conference on Information Processing in Medical Imaging*], 597–609, Springer (2017).

[16] Ghafoorian, M., Mehrtash, A., Kapur, T., Karssemeijer, N., Marchiori, E., Pesteie, M., Guttmann, C. R., de Leeuw, F.-E., Tempany, C. M., van Ginneken, B., et al., "Transfer learning for domain adaptation in mri: Application in brain lesion segmentation," in [*International Conference on Medical Image Computing and Computer-Assisted Intervention*], 516–524, Springer (2017).

[17] Çiçek, Ö., Abdulkadir, A., Lienkamp, S. S., Brox, T., and Ronneberger, O., "3d u-net: learning dense volumetric segmentation from sparse annotation," in [*International Conference on Medical Image Computing and Computer-Assisted Intervention*], 424–432, Springer (2016).

[18] Weistrand, O. and Svensson, S., "The anaconda algorithm for deformable image registration in radiotherapy," *Medical physics* **42**(1), 40–53 (2015).